Journal of Medicinal Chemistry

Article

pubs.acs.org/jmc

Structure−Activity Relationship Study of Opiorphin, a Human Dual Ectopeptidase Inhibitor with Antinociceptive Properties

Mònica Rosa,[†] Gemma Arsequell,[†] Catherine Rougeot,[‡] Luis P. Calle,[§] Filipa Marcelo,[§] Marta Pinto,[∥] Nuria B. Centeno,[∥] Jesús Jiménez-Barbero,[§] and Gregorio Valencia*[,†]

[†]Institute of Advanced Chemistry of Catalonia (IQAC-CSIC), Barcelona, Spain

[‡]Institut Pasteur-Unité de Biochimie Structurale et Cellulaire/URA2185—CNRS, Paris, France

[§]Chemical and Physical Biology, Centro de Investigaciones Biológicas (CIB-CSIC), Madrid, Spain

[∥]Computer-Assisted Drug Design Laboratory, Research Group on Biomedical Informatics (GRIB), IMIM-Universitat Pompeu Fabra, Barcelona, Spain

S *Supporting Information*

ABSTRACT: Toward developing new potential analgesics, this first structure−activity relationship study of opiorphin (H-Gln-Arg-Phe-Ser-Arg-OH), a human peptide inhibiting enkephalin degradation, was performed. A systematic Ala scanning proved that Phe[3] is a key residue for neprilysin and aminopeptidase N (AP-N) ectoenkephalinase inhibition. A series of Phe[3]-halogenated analogues revealed that halogen bonding based optimization strategies are not applicable to this residue. Additional substituted Phe[3] derivatives showed that replacing L-Phe[3] for D-Phe[3] increased the AP-N inhibition potency by 1 order of magnitude. NMR studies and molecular mechanics calculations indicated that the improved potency may be due to CH−π stacking interactions between the aromatic ring of D-Phe[3] and the Hγ protons of Arg[2]. This structural motif is not possible for the native opiorphin and may be useful for the design of further potent and metabolically stable analogues.

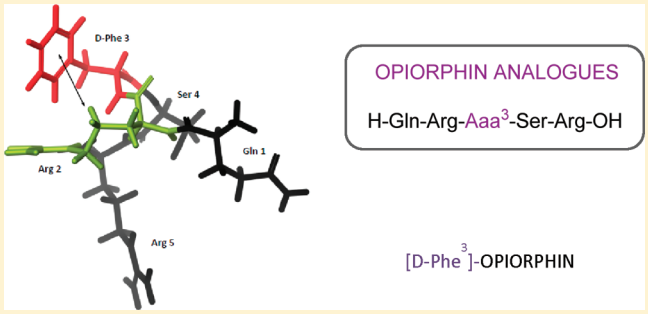

INTRODUCTION

The need for compounds with intermediate analgesic activity between nonsteroidal anti-inflammatory drugs (NSAIDs) and opioids has fueled the interest in enzyme inhibitors that protect endogenous opioid neuropeptides. One goal has been to potentiate the natural analgesic effect of the endogenous peptides Met- and Leu-enkephalin by inhibiting their enzymatic degradation. Owing to the complementary roles of both neprilysin [neutral endopeptidase (NEP), EC 3.4.24.11] and aminopeptidase N (AP-N; EC 3.4.11.2) in enkephalin inactivation, the design of dual inhibitors of these ectopeptidases seems an ideal approach.[1] Both NEP and AP-N are membrane-bound zinc metalloenzymes that belong to the M13 (NEP) and M1 (AP-N) peptidase families. Although they share a common catalytic domain, differences in the spatial arrangement of the catalytic residues and of their surroundings cause NEP to function as a carboxypeptidase that cleaves substrates at the N-terminal side of hydrophobic amino acids such as Phe, Leu, and Met, while AP-N releases the N-terminal amino acids from peptides that are not substituted α-amino acids. To date, both enzymes have escaped full experimental structural elucidation. Thus, the X-ray crystal structure of the extracellular domain (Asp52−Trp749) complexed with six different small-molecule inhibitors is the only structural information available for NEP.[2] Conversely, the structural information available for AP-N is more limited and reduced to three X-ray crystal structures corresponding to complexes of a small-molecule inhibitor with an AP-N variant from *Escherichia coli*.[3] Regrettably, human AP-N has an overall sequence identity of only 13.6% with the one fom *E. coli*.[3a] Even though homology models of human AP-N have been recently developed for designing nonpeptidic inhibitors, the authors accept that authentic structural information on the human variant would be necessary for building more accurate and useful models.[4] In spite of these caveats, the analogies of the well-studied bacterial protease thermolysin with NEP have long been used for the early designs of selective as well as dual and transition-state inhibitors of NEP and AP-N using secondary structure prediction and molecular modeling algorithms.[5] One of the first examples of such compounds is the selective NEP inhibitor thiorphan, which has led to drugs with antisecretory activity such as the antidiarrheal racecadotril (acetorphan).[6] The difficulty in formulating a dual inhibitor arises from the obvious necessity to find optimal interactions for two zinc peptidases that, despite their similarity, show different specificities. Nevertheless, mixed inhibitory products such as RB101, which is prepared by covalently linking a potent AP-N

Received: September 13, 2011
Published: January 8, 2012

dx.doi.org/10.1021/jm2012112 | *J. Med. Chem.* 2012, 55, 1181−1188

Scheme 1. Opiorphin, Ala Scan Opiorphin Analogues, and Halogenated [Phe^3]-Opiorphin Analogues

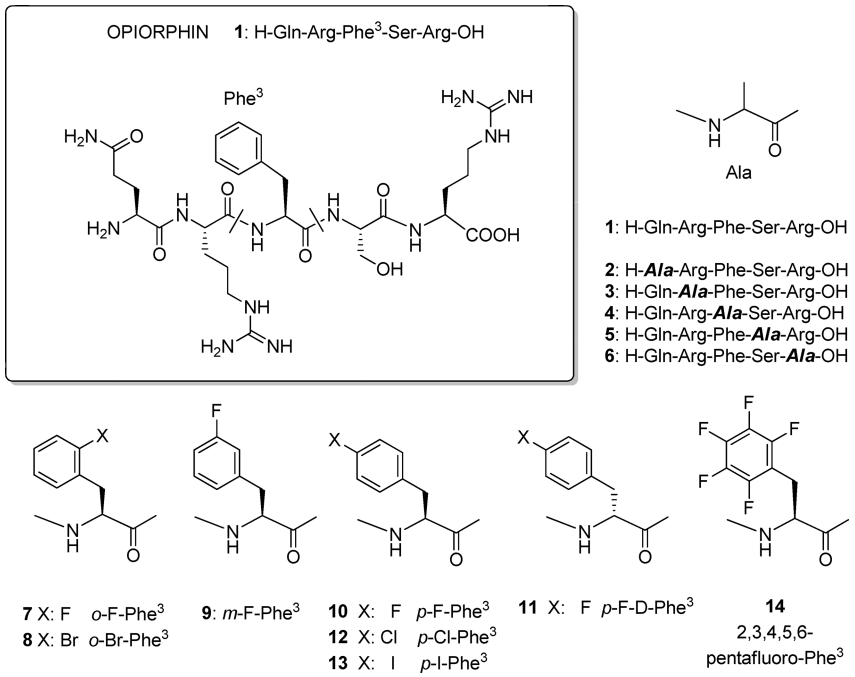

with an NEP inhibitor, have been proposed.[7] A further step in this process has been the design of single-molecule compounds such as RB3001 that are true dual inhibitors.[8] Unfortunately, none of them have yet reached clinical applications in pain management.

This search for analgesics that modulate endogenous enkephalin circulating levels has received a new impulse due to the recent discovery and isolation from mammalian sources of the peptides spinorphin (LVVYPWT)[9] and sialorphin (QHNPR).[10] These peptides, together with their human counterpart opiorphin (QRFSR),[11] which was isolated from human saliva, act as endogenous NEP and AP-N inhibitors. It has been proved that opiorphin induces antinociceptive effects in various rodent models of morphine-sensitive pain by activating endogenous enkephalin-related opioid pathways, thus demonstrating that the natural catabolism of enkephalins is physiologically regulated.[11,12] This, in turn, supports the therapeutic concept that analgesia may be amenable to enkephalin-induced potentiation by using molecules derived from naturally occcuring peptides such as opiorphin.[13] In a first exploration of this concept and toward the design of potential small-molecule peptidomimetic drugs, we have used a "ligand-based" approach to circumvent the lack of reliable structural information on these enzyme targets. Therefore, we here present our results on an Ala substitution scanning study that has revealed that Phe^3 is a crucial residue for opiorphin inhibitory activity toward both NEP and AP-N ectoenzymes. This, in turn, prompted us to conduct the first SAR study of opiorphin that is focused on Phe^3. The results show that halogen atoms placed at the aromatic function of Phe^3 are not able to induce additional stabilizing interactions with either of the two enzymes by halogen bonding. Most notably, we have found that a D-Phe for L-Phe substitution induces a 1 order of magnitude increase in AP-N inhibition potency, which can be explained by CH$-\pi$ stacking interactions between the aromatic ring of Phe^3 and the Hγ protons of Arg^2, as unveiled by NMR conformational studies in solution and molecular mechanic calculations.

RESULTS AND DISCUSSION

To gain a first insight into the most influential residues in NEP and AP-N inhibitory activity of human opiorphin, five analogues corresponding to a traditional Ala scan were synthesized (Scheme 1). The resulting peptides, as well as the other peptide derivatives reported in this paper, were prepared by solid-phase peptide synthesis techniques using standard Fmoc protocols and purified by reversed-phase liquid chromatography using a VersaFlash flash chromatography system. All the compounds were evaluated for potential inhibitory activity in vitro using commercial recombinant human NEP and AP-N soluble enzymes and synthetic fluorogenic substrates.[14−16] The monitoring of substrate hydrolysis in the presence of several concentrations of inhibitor provided kinetic plots such as those depicted in Figure 1 for the [Ala^1]-opiorphin analogue.

From these kinetic plots of enzyme inhibition, the corresponding dose-dependent inhibition curves were calculated for every compound and the two enzymes (Figure 2). Activity values expressed as EC_{50} have been extrapolated for these curves. Compounds showing EC_{50} values of over 100 μM were considered inactive, and compounds showing EC_{50} values over 70 μM very poor inhibitors.

As seen in Table 1, all the Ala-substituted analogues were inferior dual inhibitors compared to the parent opiorphin. Only the Ala for Arg^2 substitution produced an analogue slightly more potent for NEP than the parent peptide, but it was almost inactive for AP-N. The most interesting compound is **4**, which is a poor inhibitor for AP-N (IC_{50} over 70 μM) and is totally inactive against NEP (IC_{50} over 100 μM), conditions that are unique among the other compounds of Table 1. To us, **4** being the simultaneously least active compound of the series is a good indication of the relevant role played by the aromatic residue of Phe^3 in the interactions of opiorphin with both its targets, NEP

dx.doi.org/10.1021/jm2012112 | J. Med. Chem. 2012, 55, 1181−1188

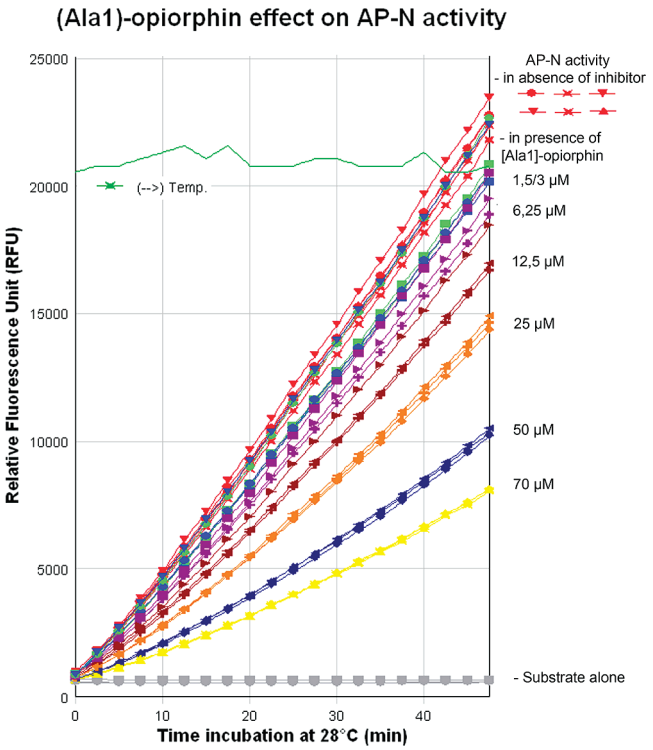

Figure 1. Fluorescence monitoring of Ala-MCA substrate hydrolysis by AP-N in the presence and absence of the [Ala^1]-opiorphin analogue. According to the conditions of initial velocity measurement, the kinetics of appearance of the fluorescent signal (RFU) were directly proportional to the rate of hydrolysis of the substrates by AP-N. The background rate of substrate autolysis representing the fluorescent signal obtained in the absence of the enzyme was subtracted to calculate the initial velocities [RFU (relative fluorescent units)/min].

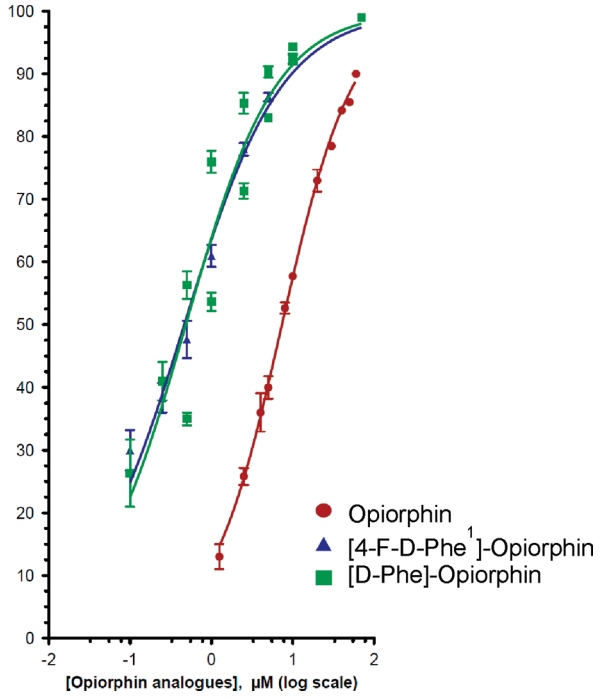

Figure 2. Dose-dependent inhibition by opiorphin (**1**), [D-Phe]-opiorphin (**15**), and [*p*-F-D-Phe]-opiorphin (**11**) of Ala-MCA substrate hydrolysis by human AP-N. Each point represents the percentage of inhibition calculated as percentage of specific velocity without inhibitor − velocity in the presence of inhibitor/velocity without inhibitor. The opiorphin analogue concentration (μM) is plotted on a log scale.

and AP-N, and therefore was considered a good target for an SAR study.

First, given the critical role of Phe^3 in the inhibitory potency of opiorphin toward NEP and AP-N, and that this aromatic side chain residue is a suitable structural motif for the introduction of halogen atoms, we sought to improve the inhibitory properties of opiorphin by applying the halogen bonding rationale. This approach is based on the ability of halogen atoms to function as general, effective, and reliable sites for directing molecular recognition processes.[17] The fact that about half of the molecules currently entering high-throughput screening tests are halogenated highlights the importance of this concept for drug design.[18] Thus, a suitable set of commercial Phe building blocks with halogen atoms in their side chains were chosen and the corresponding opiorphin analogues prepared and tested (Scheme 1).

As Table 2 reflects, none of the seven halogenated compounds assayed (**7**−**13**) were more potent dual NEP and AP-N inhibitors than the parent opiorphin. Moreover, in the homologous series of halogenated analogues at the *para* position (**10**, **12**, **13**), activities did not gradually increase with the atomic weight of the halogen atom (F vs Cl vs I). A similar situation is suggested by the shortest *ortho*-halogenated series (**7**, **8**) (F vs Br). This evidence supports that *ortho* and *para* halogenation of Phe^3 does not generate new stabilizing interactions mediated by halogen bonds between opiorphin and the two enzymes. Fluorination at *meta* (**9**) and perfluorination of Phe^3 (**14**) totally prevent enzymatic inhibition.

Table 1. Inhibition of hAP-N and hNEP Activities by Opiorphin and Ala Analogues

peptide	compound	sequence	hAP-N IC_{50} ± SD (μM)	hNEP-endoP IC_{50} ± SD (μM)
1	opiorphin	H-Gln-Arg-Phe-Ser-Arg-OH	8.1 ± 0.1	30 ± 3
2	[Ala^1]-opiorphin	H-*Ala*-Arg-Phe-Ser-Arg-OH	37 ± 3	>70
3	[Ala^2]-opiorphin	H-Gln-*Ala*-Phe-Ser-Arg-OH	65 ± 3	12 ± 1
4	[Ala^3]-opiorphin	H-Gln-Arg-*Ala*-Ser-Arg-OH	>70	≫100
5	[Ala^4]-opiorphin	H-Gln-Arg-Phe-*Ala*-Arg-OH	47 ± 2	39 ± 2
6	[Ala^5]-opiorphin	H-Gln-Arg-Phe-Ser-*Ala*−OH	>70	33 ± 2

To further examine the role of Phe^3 in opiorphin activity, a second series of analogues, in which Phe^3 was substituted by Phe isomers, derivatives, and mimics that have been chosen because they are commonly used for SAR studies of other naturally occurring peptides[19,20] and their corresponding building blocks are commercially available, were prepared and tested against both NEP and AP-N activities (Scheme 2). A further criterion for this selection was to preliminarily see if substitutions possibly leading to enzymatic resistance such as L by D and α by β changes on the configuration of this amino acid have an effect on the biological activity of opiorphin. The Bpa

dx.doi.org/10.1021/jm2012112 | J. Med. Chem. 2012, 55, 1181−1188

Table 2. Inhibition of hAP-N and hNEP Activities by Opiorphin and Halogenated Phe[3] Analogues

peptide	name	compound	hAP-N IC_{50} ± SD (μM)	hNEP-endoP IC_{50} ± SD (μM)
1	opiorphin	H-Gln-Arg-Phe-Ser-Arg-OH	8.1 ± 0.1	30 ± 3
7	[*o*-F-Phe[3]]-opiorphin	H-Gln-Arg-*(o-F)Phe*-Ser-Arg-OH	44 ± 3	48 ± 3
8	[*o*-Br-Phe[3]]-opiorphin	H-Gln-Arg-*(o-Br)Phe*-Ser-Arg-OH	65 ± 4	30 ± 2
9	[*m*-F-Phe[3]]-opiorphin	H-Gln-Arg-*(m-F)Phe*-Ser-Arg-OH	>100	>100
10	[*p*-F-Phe[3]]-opiorphin	H-Gln-Arg-*(p-F)Phe*-Ser-Arg-OH	13.5 ± 0.5	>100
11	[*p*-F-D-Phe[3]]-opiorphin	H-Gln-Arg-*(p-F)*-D-*Phe*-Ser-Arg-OH	0.5 ± 0.1	>100
12	[*p*-Cl-Phe[3]]-opiorphin	H-Gln-Arg-*(p-Cl)Phe*-Ser-Arg-OH	48 ± 5	70 ± 10
13	[*p*-I-Phe[3]]-opiorphin	H-Gln-Arg-*(p-I)Phe*-Ser-Arg-OH	30 ± 3	>100
14	[2,3,4,5,6-pentafluoro-Phe[3]]-opiorphin	H-Gln-Arg-*(2,3,4,5,6-pentafluoro)Phe*-Ser-Arg-OH	≫100	>100

Scheme 2. [Phe[3]]-Opiorphin Analogues

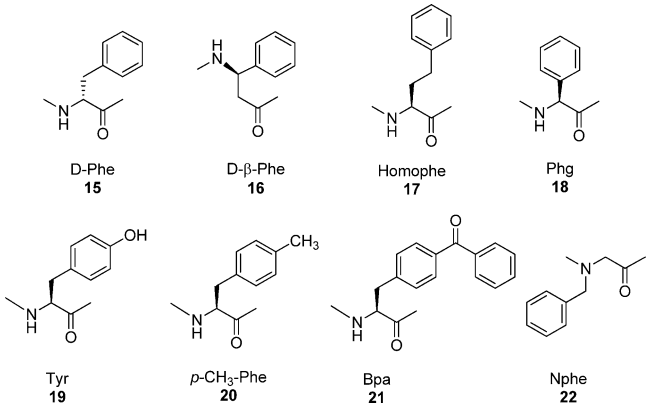

substitution (**21**) was screeened in view of future photoaffinity labeling experiments.

As seen from their EC_{50} values (Table 3), none of the eight compounds (**15**−**21**) are dual NEP and AP-N inhibitors. Also, small structural changes (i.e., Homophe, Phg, and Tyr for Phe[3]) (**17**, **18**, **19**) drastically affected NEP inhibition while still preserving some AP-N inhibition. The most notable finding was that [D-Phe[3]]-opiorphin is 1 order of magnitude more potent than opiorphin in AP-N inhibition. This substitution even tolerates *para* fluorination, as the resulting compound displays similar AP-N inhibitory potency.

To rationalize these observations from a structural perspective, solution NMR studies were then performed. Using standard 2D NMR methods, chemical shift assignments for the natural peptide opiorphin and for a subset of the analogues were collected (Table S2, Supporting Information). Analysis of these data mainly served to verify the different tendencies of natural [L-Phe[3]]-opiorphin with respect to its D-Phe[3] analogue. On the other hand, no significant differences were appreciated between the fluorine-containing derivatives and the parent compound.

On a first inspection, the ^{1}H NMR spectra of the peptides containing D-Phe showed that the ^{1}H signals were more

Table 3. Inhibition of hAP-N and hNEP Activities by Opiorphin and Other Phe[3] Analogues

	name	compound	hAP-N IC_{50} ± SD (μM)	hNEP-endoP IC_{50} ± SD (μM)
1	opiorphin	H-Gln-Arg-Phe-Ser-Arg-OH	8.1 ± 0.1	30 ± 3
15	[D-Phe[3]]-opiorphin	H-Gln-Arg-D-*Phe*-Ser-Arg-OH	0.5 ± 0.1	≫100
11	[*p*-F-D-Phe[3]]-opiorphin	H-Gln-Arg-*(p-F)*-D-*Phe*-Ser-Arg-OH	0.5 ± 0.1	>100
16	[D-*β*-Phe[3]]-opiorphin	H-Gln-Arg-D-*β-Phe*-Ser-Arg-OH	>70	≫100
17	[Homophe[3]]-opiorphin	H-Gln-Arg-*Homophe*-Ser-Arg-OH	54 ± 10	70 ± 10
18	[Phg[3]]-opiorphin	H-Gln-Arg-*Phg*-Ser-Arg-OH	10 ± 3	≫100
19	[Tyr[3]]-opiorphin	H-Gln-Arg-*Tyr*-Ser-Arg-OH	64 ± 5	70 ± 10
20	[*p*-Me-Phe[3]]-opiorphin	H-Gln-Arg-*(p-Me)Phe*-Ser-Arg-OH	45 ± 4	>100
21	[Bpa[3]]-opiorphin	H-Gln-Arg-*Bpa*-Ser-Arg-OH	30 ± 3	>100
22	[Nphe[3]]-opiorphin	H-Gln-Arg-*Nphe*-Ser-Arg-OH	≫100	≫100

dispersed than those containing the natural L-Phe residue. In a more quantitative analysis, the chemical shift indexes (CSIs)[21] were calculated, which measure the deviation of the different backbone α protons (Hα) from the typical random coil values (Figure S1 and Table S3, Supporting Information). However, the most remarkable structural differences between the opiorphin analogues and the natural compound were observed when comparing the D-Phe versus L-Phe analogues due to the different β-sheet-forming propensity of Arg[2]. The chemical-shift-based evidence for these differences was obtained by measuring the values of the key coupling constant $^3J_{NH,H\alpha}$ for Arg[2] on these epimeric peptides. Thus, for instance, the value of $^3J_{NH,H\alpha}$ measured for [*p*-F-Phe[3]]-opiorphin was 6.9 Hz, while for the corresponding [D-Phe[3]]-opiorphin analogue it decreased to 5.4 Hz. An additional difference concerning the Arg[2] residues was that the Hγ protons of the D-Phe peptides were significantly shielded with respect to their L-Phe[3] counterparts (Table S1, Supporting Information). In particular, the R2 Hγ2 and Hγ3 protons of [*p*-F-D-Phe[3]]-opiorphin appeared shielded at a higher field, −0.38 and −0.52 ppm, respectively, than those of the L-Phe analogue ([*p*-F-Phe[3]]-opiorphin).

At this point, taking into account this experimental evidence, molecular mechanics calculations were performed to construct a 3D model. Thus, 3D structures for the natural opiorphin peptide and its corresponding [D-Phe[3]]-opiorphin analogue were generated by employing a conformational search protocol with Macromodel,[22] as integrated in the Maestro package.[23] As expected from their small size, different minima were found for these two peptides. However, for the D-Phe[3] derivative, the global minimum presented spatial proximity between the D-Phe[3] aromatic ring and the Hγ protons of Arg[2], a fact that supports the experimental chemical shift evidence (Figure 3). This geometry is also in agreement with the experimental coupling constants that define the orientation of D-Phe[3], that is, $^3J_{H\alpha,H\beta2}$ and $^3J_{H\alpha,H\beta3}$ (4.6 and 11.3 Hz, respectively). Only in this calculated orientation does the aromatic ring adopt the proper presentation to provide CH−π stacking interactions with the Hγ protons at the arginine side chain. The observed

dx.doi.org/10.1021/jm2012112 | J. Med. Chem. 2012, 55, 1181−1188

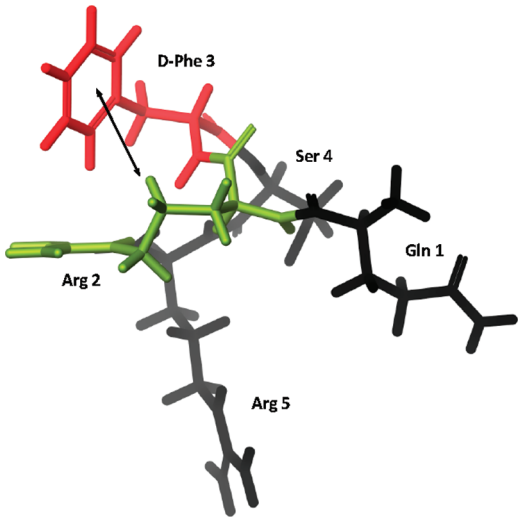

Figure 3. Model structure of the [D-Phe^3]-opiorphin peptide (**15**) showing the eventual interaction between the Hγ protons of Arg^2 (in green) and D-Phe^3 (in red).

nuclear Overhauser effect (NOE) contacts also support the prevalent existence of this conformation, defined by a χ_1(NH−Cα−Cβ−C$_{ar}$) value of around −60°.

In contrast to the D-Phe^3 analogue, key NMR experimental data such as coupling constants and NOEs for the native opiorphin are consistent with the existence of a different conformation for the corresponding side chain of Phe^3, with a χ_1(NH−Cα−Cβ−C$_{ar}$) value of around 180°. Notably, this geometry does not allow the formation of CH−π stacking interactions with the Hγ protons of Arg^2. According to molecular mechanics calculations, this undetected conformation, which would permit the π-cation, would be strongly destabilized in energy terms. Moreover, the expected $^3J_{H\alpha,H\beta2}$ and $^3J_{H\alpha,H\beta3}$ coupling constants for this geometry should have small values, in contrast with those observed experimentally (one small and one large value of 9.6 Hz, respectively).

Finally, the 3D structures that in our hands best fit the experimental NMR data for opiorphin and its corresponding D-Phe^3 analogue are presented in Figure 4. These conformers were validated by the presence of a significant number of experimental NOE contacts. In particular, the 3D structure proposed for the synthetic [D-Phe^3]-opiorphin analogue satisfactorily explains three interresidual contacts (NH-F3/NH-S4, NH-R5/Hβs-S4, and NH-F3/Hβs-R2). In contrast, the NOE pattern observed for natural opiorphin permits the postulation of a different spatial orientation of these residues. The most noticeable differences between both molecules are observed for the NH-R5/Hβs-S4 and NH-F3/NH-S4 NOEs. In summary, the different spatial architectures of these two peptides, which originate from the relative presentations of Arg^2 and Phe^3 residues, translate into the rather distinct electrostatic potential energy surface plots of these molecules that may be at the origin of the differential properties discussed above.

CONCLUSIONS

An alanine scanning study of opiorphin has provided evidence that an Ala^3 for Phe^3 substitution produces the least active analogue, thus indicating the relevant role that this aromatic residue may play in opiorphin binding activity and specificity toward both targets, NEP and AP-N. In an attempt to apply the halogen bonding rationale to improve the biological properties of opiorphin through Phe^3 halogenation, we found that *ortho* and *para* halogenation of the Phe^3 aromatic ring does not result in opiorphin activity potentiation by new halogen bonding stabilizing interactions. Also, fluorination at *meta* and perfluorination completely block its enzyme inhibition activity. A further preparation of a series of substituted Phe^3 derivatives has shown that substitution of L-Phe^3 by D-Phe^3 increases the AP-N inhibition potency of opiorphin by 1 order of magnitude while depleting its NEP inhibition activity. Comparative conformational studies in solution by NMR and molecular mechanics calculations have shown that the observed AP-N inhibition potency enhancement may be due to CH−π stacking interactions between the aromatic ring of Phe^3 and the Hγ protons of Arg^2, which can take place only in the D-Phe^3 analogue. This first SAR study on opiorphin has failed to render a more potent opiorphin-based dual NEP and AP-N inhibitor but has identified a strategy to boost its AP-N inhibition potency by simultaneously providing analogues more metabolically stable than the native peptide.

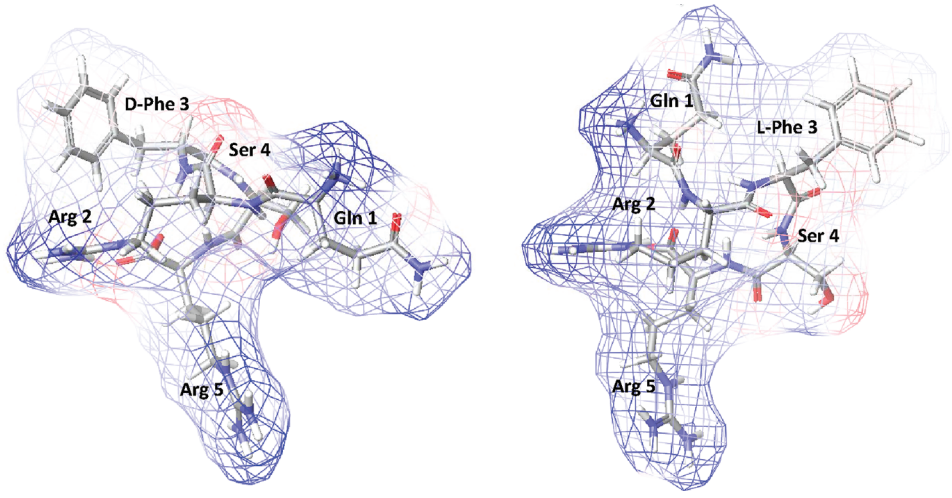

Figure 4. Electrostatic potential energy surface plots for the modified [D-Phe^3]-opiorphin peptide (**15**) (left) and the natural opiorphin peptide (**1**) (right).

dx.doi.org/10.1021/jm2012112 | *J. Med. Chem.* 2012, 55, 1181−1188

EXPERIMENTAL SECTION

Materials. All amino acid building blocks, coupling reagents, and derivatized resins (Fmoc-Ala Wang resin, Fmoc-Arg(Pmc) Wang resin) were purchased from Novabiochem AG. ACS grade organic solvents and other reagents such as sodium dodecyl sulfate-d_{25} were purchased from Sigma-Aldrich. All other reagents used were of analytical grade.

Peptide Synthesis. Opiorphin (**1**) and the peptide analogues **2**–**22** were synthesized manually by using standard N^{α}-Fmoc solid-phase methodology on either Fmoc-Ala-prederivatized Wang resin or Fmoc-Arg(Pmc)-prederivatized Wang resin.[24] N^{α}-Fmoc-protected amino acids (3 equiv) were used. The side chain protecting groups used to build the peptide sequences were the following: Trt for Gln and Asn, *t*-Bu for Ser and Thr, Boc for Lys, and Pmc for Arg. The Fmoc-Arg(Pmc) Wang resin (1 equiv) was placed in a glass peptide synthesis column with a frit on the bottom and swollen in DMF for 1 h. The amide couplings were effected by DIC (3 equiv) and HOBt (6 equiv). In the case of Fmoc-Gln(Trt)OH, couplings were effected using PyBOP (3 equiv), HOBt (3 equiv), and DIEA (6 equiv). Each coupling was performed manually in this peptide synthesis column using DMF as a solvent under reciprocal oscillating agitation. The coupling efficiencies were monitored by the Kaiser ninhydrin test. The Fmoc groups were removed with a solution of 20% piperidine in DMF (1×9 min). The deprotected resin was washed with DMF, DCM, and then DMF. After assembly of the peptide sequence, a cocktail of TFA/TIS/H_2O (95:2.5:2.5) was used to remove the side chain protecting groups and to cleave the peptide from the resin. The crude peptides were precipitated with ice-cold *tert*-butyl methyl ether, filtered, redissolved in water, and lyophilized. The final peptides were purified on a reversed-phase (C-18) column with the VersaFlash flash chromatography system using a H_2O–ACN gradient. The homogeneity and identity of the final peptides were determined by analytical RP-HPLC and HRMS on a Waters UPLC-ESI/TOF system. All the obtained final peptides showed >98% purity. The purified peptides were characterized by high-resolution mass spectroscopy, TLC, analytical HPLC, and ^{1}H NMR (see the Supporting Information).

NMR Spectroscopy. All experiments were recorded in H_2O/D_2O (90:10) on a Bruker Avance 600 MHz instrument equipped with a triple-channel cryoprobe and at 278 K. NMR assignments were accomplished using standard 2D TOCSY experiments at different mixing times (20 and 60 ms) and 2D NOESY experiments (300 ms). The resonance of 2,2,3,3-tetradeuterio-3-(trimethylsilyl)propionic acid (TSP) was used as a chemical shift reference in the ^{1}H NMR experiments [δ(TSP) = 0 ppm].

Initial NMR experiments for the natural peptide opiorphin were carried out to optimize the experimental conditions. The same methodology was then applied to the other analogues containing Phe[3] amino acid modifications.

Structure Determination. Molecular mechanics were conducted using Macromodel 9.6,[22] as implemented in version 8.5.110 of the Maestro suite,[23] using OPLS-2005* [25] as the force field. The starting coordinates for conformational search calculations (OPLS-2005 as the force field) were those obtained after energy minimization for both L- and D-Phe[3] analogues. The continuum GB/SA solvent model[26] was employed, and the general PRCG (Polak–Ribiere conjugate gradient) method for energy minimization was used. A conformational search protocol was then performed, using the Monte Carlo torsional sampling (MCMM) method, with the same force field and minimization conditions.

Determination of Biological Activities: Measurement of NEP and AP-N Activities Using Fluorimetric Assays. *Reagents.* Recombinant human NEP and human AP-N (devoid of their respective N-terminal cytosol and transmembrane segment) were purchased from R&D Systems and used as pure sources of ectopeptidases. Abz-dRGL-(EDDnp) FRET peptide (Abz = *o*-aminobenzoic acid; EDDnp = *N*-(2,4-dinitrophenyl)ethylenediamine), that is, an internally quenched fluorescent substrate specific for NEP-endopeptidase activity, was synthesized by Thermo-Fisher Scientific (Germany). Alanine-MCA (Ala-MCA), a fluorogenic substrate for measuring aminopeptidase activity, was purchased from Sigma.

Measurement of hNEP-Ectopeptidase Activity. Using a black half-area 96-well microplate, the standard reaction mixture consisted of the enzyme in 100 mM Tris–HCl, pH 7, containing 200 mM NaCl (100 μL final volume). The substrate was added after preincubation for 10 min at 28 °C, and the kinetics of appearance of the fluorescent signal (RFU) were directly analyzed over 40 min at 28 °C using a fluorimeter microplate reader (monochromator Infinite 200-Tecan) at 320 and 420 nm excitation and emission wavelengths, respectively.

Measurement of hAP-N-Ectopeptidase Activity. The standard reaction mixture consisted of the enzyme in 100 mM Tris–HCl, pH 7.0 (100 μL final volume). The Ala-MCA substrate was added after preincubation for 10 min at 28 °C, and the kinetics of appearance of the signal were monitored for 40 min at 28 °C by using the fluorimeter reader at 380 nm excitation and 460 nm emission wavelengths.

ASSOCIATED CONTENT

Supporting Information

^{1}H NMR, HRMS, FRET fluorescence monitoring, and NMR data of opiorphin and its corresponding analogues. This material is available free of charge via the Internet at http://pubs.acs.org.

AUTHOR INFORMATION

Corresponding Author

*Phone: +34934006113. Fax: +34 932045904. E-mail: gregorio.valencia@iqac.csic.es.

ACKNOWLEDGMENTS

This work was supported by a grant from the Fundació Marató de TV3 (Pain, Project Reference 070430-31-32-33). We thank F. J. Cañada for helpful discussions. J.J.-B. acknowledges financial support from the Ministerio de Ciencia e Innovación (Spain) (Grant CTQ2009-08536). F.M. thanks FCT-Portugal for a postdoctoral research grant (SFRH/BPD/65462/2009). M.R. acknowledges a fellowship (Grant AP2009-2534, Formación de Profesorado Universitario) from the Ministry of Education.

ABBREVIATIONS USED

Abz, *o*-aminobenzoic acid; *β*-D-Phe, (*S*)-3-amino-3-phenylpropionic acid or D-*β*-phenylalanine; Boc, *tert*-butoxycarbonyl; ACN, acetonitrile; Bpa, *p*-benzoylphenylalanine; CSI, chemical shift index; DCM, dichloromethane; DIC, *N*,*N*′-diisopropylcarbodiimide; DIEA, *N*,*N*-diisopropylethylamine; DMF, *N*,*N*-dimethylformamide; Dnp, 2,4-dinitrophenyl; Fmoc, (fluoren-9-ylmethoxy)carbonyl; Fmoc-L-Ala Wang resin, N^{α}-Fmoc-L-alanine 4-(benzyloxy)benzyl ester polymer-bound; Fmoc-L-Arg(Pmc) Wang resin, N^{α}-Fmoc-N^{δ}-Pmc-L-arginine 4-(benzyloxy)benzyl ester polymer-bound; hAP-N, human aminopeptidase N; hNEP, human neprilysin; Homophe, homophenylalanine; MCMM, Monte Carlo torsional sampling method; MCA, methoxycoumarin; NMR, nuclear magnetic resonance; Nphe, *N*-benzylglycine; NOESY, nuclear Overhauser enhancement spectroscopy; Phg, phenylglycine; Pmc, 2,2,5,7,8-pentamethylchroman-6-sulfonyl; PyBOP, (benzotriazol-1-yloxy)trispyrrolidinophosphonium hexafluorophosphate; rmsd, root-mean-square deviation; RFU, relative fluorescence unit; RP-LC, reversed-phase liquid chromatography (VersaFlash flash chromatography system); SAR, structure–activity relationship; SPPS, solid-phase peptide synthesis; *t*-Bu, *tert*-butyl; TFA, trifluoroacetic acid; TIS, triisopropylsilane;

TOCSY, total correlation spectroscopy; Trt, trityl; TSP, 2,2,3,3-tetradeuterio-3-(trimethylsilyl)propionic acid[27]

REFERENCES

(1) (a) Roques, B. P. Novel approaches to targeting neuropeptide systems. *Trends Pharmacol. Sci.* **2000**, *21*, 475−483. (b) Noble, F; Roques, B. P. Protection of endogenous enkephalin catabolism as natural approach to novel analgesic and antidepressant drugs. *Expert Opin. Ther. Targets* **2007**, *11*, 145−159.

(2) (a) Oefner, C.; D'Arcy, A.; Hennig, M.; Winkler, F. K.; Dale, G. E. Structure of human neutral endopeptidase (Neprilysin) complexed with phosphoramidon. *J. Mol. Biol.* **2000**, *296*, 341−349. (b) Oefner, C.; Roques, B. P.; Fournié-Zaluski, M. C.; Dale, G. E. Structural analysis of neprilysin with various specific and potent inhibitors. *Acta Crystallogr., D: Biol. Crystallogr.* **2004**, *60*, 392−396. (c) Oefner, C.; Pierau, S.; Schulz, H.; Dale, G. E. Structural studies of a bifunctional inhibitor of neprilysin and DPP-IV. *Acta Crystallogr., D: Biol. Crystallogr.* **2007**, *63*, 975−981. (d) Sahli, S.; Frank, B.; Schweizer, W. B.; Diederich, F.; Blum-Kaelin, D.; Aebi, J. D.; Böhm, H. J. Second-generation inhibitors for the metalloprotease neprilysin based on bicyclic heteroaromatic scaffolds: synthesis, biological activity, and X-ray crystal-structure analysis. *Helv. Chem. Acta* **2005**, *88*, 731−750.

(3) (a) Ito, K.; Nakajima, Y.; Onohara, Y.; Takeo, M.; Nakashima, K.; Matsubara, F.; Ito, T.; Yoshimoto, T. Crystal structure of amino-peptidase N (proteobacteria alanyl aminopeptidase) from *Escherichia coli* and conformational change of methionine 260 involved in substrate recognition. *J. Biol. Chem.* **2006**, *281*, 33664−33676. (b) Fournié-Zaluski, M. C.; Poras, H.; Roques, B. P.; Nakajima, Y.; Ito, K.; Yoshimoto, T. Structure of aminopeptidase N from *Escherichia coli* complexed with the transition-state analogue aminophosphinic inhibitor PL250. *Acta Crystallogr., D: Biol. Crystallogr.* **2009**, *65*, 814−822.

(4) Albrecht, S.; Al-Lakkis-Wehbe, M.; Orsini, A; Defoin, A.; Pale, P.; Salomon, E.; Tarnus, C.; Weibel, J. M. Amino-benzosuberone: a novel warhead for selective inhibition of human aminopeptidase-N/CD13. *Bioorg. Med. Chem.* **2011**, *19*, 1434−1449.

(5) (a) Matthews, B. W. Structural basis of thermolysin and related zinc peptidases. *Acc. Chem. Res.* **1988**, *21*, 333−340. (b) Roques, B. P. Zinc metallopeptidases: active site structure and design of selective and mixed inhibitors—new approaches in the search for analgesics and antihypertensives. *Biochem. Soc. Trans.* **1999**, *21*, 678−685. (c) Roques, B. P.; Noble, F.; Daugé, V.; Fournié-Zaluski, M. C.; Beaumont, A. Neutral endopeptidase 24.11: structure, inhibition, and experimental and clinical pharmacology. *Pharmacol. Rev.* **1993**, *45*, 87−146.

(6) (a) Matheson, A. J.; Noble, S. Racecadotril. *Drugs* **2000**, *59*, 829−835. (b) Spillantini, M. G.; Geppetti, P.; Fanciullacci, M.; Michelacci, S.; Lecomte, J. M.; Sicuteri, F. *In vivo* 'enkephalinase' inhibition by acetorphan in human plasma and CSF. *Eur. J. Pharmacol.* **1986**, *125*, 147−150. (c) Reggiani, A.; Carenzi, A.; Frigeni, V.; Della Bella, D. Effect of bestatin and thiorphan on [Met^5]enkephalin-Arg^6-Phe^7-induced analgesia. *Eur. J. Pharmacol.* **1984**, *105*, 361−364.

(7) (a) Jutkiewicz, E. M. RB101-mediated protection of endogenous opioids: potential therapeutic utility? *CNS Drug Rev.* **2007**, *13*, 192−205. (b) Fournié-Zaluski, M. C.; Coric, P.; Turcaud, S.; Lucas, E.; Noble, F.; Maldonado, R.; Roques, B. P. "Mixed inhibitor−prodrug" as a new approach toward systemically active inhibitors of enkephalin-degrading enzymes. *J. Med. Chem.* **1992**, *35*, 2474−2481. (c) Roques, B. P.; Noble, F.; Daugé, V.; Fournié-Zaluski, M. C.; Beaumont, A. Neutral endopeptidase 24.11: structure, inhibition, and experimental and clinical pharmacology. *Pharmacol. Rev.* **1993**, *45*, 87−146.

(8) (a) Chen, H.; Noble, F.; Mothé, A.; Meudal, H.; Coric, P.; Danascimento, S.; Roques, B. P.; George, P.; Fournié-Zaluski, M. C. Phosphinic derivatives as new dual enkephalin degrading enzyme inhibitors: synthesis, biological properties, and antinociceptive activities. *J. Med. Chem.* **2000**, *43*, 1398−1408. (b) Chen, H.; Noble, F.; Coric, P.; Fournie-Zaluski, M. C.; Roques, B. P. Aminophosphinic inhibitors as transition state analogues of enkephalin-degrading enzymes: a new class of central analgesics. *Proc. Natl. Acad. Sci. U.S.A.* **1998**, *95*, 12028−12033.

(9) (a) Yamamoto, Y.; Ono, H.; Ueda, A.; Shimamura, M.; Nishimura, K.; Hazato, T.. Spinorphin as an endogenous inhibitor of enkephalin-degrading enzymes: roles in pain and inflammation. *Curr. Protein Pept. Sci.* **2002**, *3*, 587−599. (b) Nishimura, K.; Hazato, T. Isolation and identification of an endogenous inhibitor of enkephalin-degrading enzymes from bovine spinal cord. *Biochem. Biophys. Res. Commun.* **1993**, *194*, 713−719.

(10) Rougeot, C.; Messaoudi, M.; Hermitte, V.; Rigault, A. G.; Blisnick, T.; Dugave, C.; Desor, D.; Rougeon, F. Sialorphin, a natural inhibitor of rat membrane-bound neutral endopeptidase that displays analgesic activity. *Proc. Natl. Acad. Sci. U.S.A.* **2003**, *100*, 8549−8554.

(11) Wisner, A.; Dufour, E.; Messaoudi, M.; Nejdi, A.; Marcel, A.; Ungeheuer, M. N.; Rougeot, C. Human opiorphin, a natural antinociceptive modulator of opioid-dependent pathways. *Proc. Natl. Acad. Sci. U.S.A.* **2006**, *103*, 17979−17984.

(12) (a) Tian, X. Z.; Chen, J.; Xiong, W.; He, T.; Chen, Q. Effects and underlying mechanisms of human opiorphin on colonic motility and nociception in mice. *Peptides* **2009**, *30*, 1348−1354. (b) Rougeot, C.; Robert, F.; Menz, L.; Bisson, J. F.; Messaoudi, S. Systemically active human opiorphin is a potent yet non-addictive analgesic without drug tolerance effects. *J. Physiol. Pharmacol.* **2010**, *61*, 483−490. (c) Javelot, H. M.; Messaoudi, S.; Garnier, S.; Rougeot, C. Human opiorphin is a naturally occurring antidepressant acting selectively on enkephalin-dependent delta-opioid pathways. *J. Physiol. Pharmacol.* **2010**, *61*, 355−362. (d) Yang, Q. Z.; Lu, S. S.; Tian, X. Z.; Yang, A. M.; Ge, W. W.; Chen, Q. The antidepressant-like effect of human opiorphin via opioid-dependent pathways in mice. *Neurosci. Lett.* **2011**, *489*, 131−135.

(13) Rougeot, C. Opiorphin peptide derivatives as potent inhibitors of enkephalin-degrading ectopeptidases. PCT/EP2009/054171, April 4, 2009; WO/2009/124948, Oct 15, 2009.

(14) (a) Medeiros, M. A.; França, M. S.; Boileau, G.; Juliano, L.; Carvalho, K. M. Specific fluorogenic substrates for neprilysin (neutral endopeptidase, EC 3.4.24.11) which are highly resistant to serine- and metalloproteases. *Braz. J. Med. Biol. Res.* **1997**, *30*, 1157−1162. (b) Barros, N. M.; Campos, M.; Bersanetti, P. A.; Oliveira, V.; Juliano, M. A.; Boileau, G.; Juliano, L.; Carmona, A. K. Neprilysin carboxydipeptidase specificity studies and improvement in its detection with fluorescence energy transfer peptides. *Biol. Chem.* **2007**, *388*, 447−455.

(15) Rougeot C. Method for identifying BPLP and opiorphin agonists or antagonists. PCT/EP2009/050567, Jan 19, 2009; WO/2009/090265, July 23, 2009.

(16) (a) Mantle, D.; Hardy, M. F.; Lauffart, B.; McDermott, J. R.; Smith, A. I.; Pennington, R. J. Purification and characterization of the major aminopeptidase from human skeletal muscle. *Biochem. J.* **1983**, *211*, 567−573. (b) Abid, K.; Rochat, B.; Lassahn, P. G.; Stöcklin, R.; Michalet, S.; Brakch, N.; Aubert, J. F.; Vatansever, B.; Tella, P.; De Meester, I.; Grouzmann, E. Kinetic study of neuropeptide Y (NPY) proteolysis in blood and identification of NPY3−35: a new peptide generated by plasma kallikrein. *J. Biol. Chem.* **2009**, *284*, 24715−24724.

(17) (a) Parisini, E.; Metrangolo, P.; Pilati, T.; Resnati, G.; Terraneo, G. Halogen bonding in halocarbon-protein complexes: a structural survey. *Chem. Soc. Rev.* **2011**, *40*, 2267−227. (b) Hardegger, L. A.; Kuhn, B.; Spinnler, B.; Anselm, L.; Ecabert, R.; Stihle, M.; Gsell, B.; Thoma, R.; Diez, J.; Benz, J.; Plancher, J. M.; Hartmann, G.; Banner, D. W.; Haap, W.; Diederich, F. Systematic investigation of halogen bonding in protein-ligand interactions. *Angew. Chem., Int. Ed.* **2011**, *50*, 314−318.

(18) Ibrahim, M. A. Molecular mechanical study of halogen bonding in drug discovery. *J. Comput. Chem.* **2011**, *32*, 2564−2574.

(19) Guerrini, R.; Caló, G.; Bigoni, R.; Rizzi, D.; Rizzi, A.; Zucchini, M.; Varani, K.; Hashiba, E.; Lambert, D. G.; Toth, G.; Borea, P. A.; Salvadori, S.; Regoli, D. Structure−activity studies of the Phe(4) residue of nociceptin(1−13)-NH(2): identification of highly potent agonists of the nociceptin/orphanin FQ receptor. *J. Med. Chem.* **2001**, *44*, 3956−3964.

(20) Shao, X.; Gao, Y.; Zhu, C.; Liu, X.; Yao, J.; Cui, Y.; Wang, R. Conformational analysis of endomorphin-2 analogs with phenylalanine

mimics by NMR and molecular modeling. *Bioorg. Med. Chem.* **2007**, *15*, 3539−3547.
(21) Wishart, D. S.; Bigam, C. G.; Holm, A.; Hodges, R. S.; Sykes, B. D. ^{1}H, ^{13}C and ^{15}N random coil NMR chemical shifts of the common amino acids. I. Investigations of nearest-neighbor effects. *J. Biomol. NMR* **1995**, *5*, 67−81.
(22) *MacroModel*, version 9.6; Schrödinger, LLC: New York, 2008.
(23) *Maestro, a Powerful All-Purpose Molecular Modeling Environment*, version 8.5; Schrödinger, LLC: New York, 2008.
(24) Chan, W. C.; White, P. D. In *Fmoc Solid Phase Peptide Synthesis: A Practical Approach*; Chan, W.C., White, P.D., Eds.; Oxford University Press: Oxford, U.K., 2000; pp 41−76.
(25) Jorgensen, W. L.; Maxwell, D. S.; Tirado-Rives, J. Development and testing of the OPLS all-atom force field on conformational energetics and properties of organic liquids. *J. Am. Chem. Soc.* **1996**, *118*, 11225−11236.
(26) Still, W. C.; Tempczyk, A.; Hawley, R. C.; Hendrickson, T.. Semianalytical treatment of solvation for molecular mechanics and dynamics. *J. Am. Chem. Soc.* **1990**, *112*, 6127−6129.
(27) Abbreviations used for amino acids and designation of peptides follow the rules of the IUPAC-IUB Commission of Biochemical Nomenclature in *J. Biol. Chem.* **1972**, *247*, 977−983.